Analyst

Accepted Manuscript

This article can be cited before page numbers have been issued, to do this please use: J. lv, S. Xie, W. Cai, J. Zhang, D. Tang and Y. Tang, *Analyst*, 2017, DOI: 10.1039/C7AN01306J.

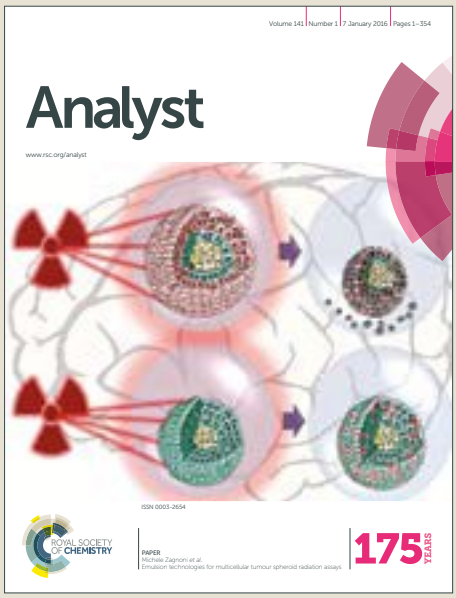

View Article Online
DOI: 10.1039/C7AN01306J

Analyst

ARTICLE

Highly Effective Target Converting Strategy for Ultrasensitive Electrochemical Assay of Hg^{2+}

Received 00th January 20xx,
Accepted 00th January 20xx

DOI: 10.1039/x0xx00000x

www.rsc.org/

Jin Lv,[a,b] Shunbi Xie,[a,*] Wei Cai,[a,b] Jin Zhang,[a,b] Dianyong Tang[a] and Ying Tang[a,*]

An electrochemical sensing system based on highly effective mercuric ion (Hg^{2+}) converting strategy and rolling circle amplification (RCA) has been developed for Hg^{2+} ultrasensitive detection. The Hg^{2+} converting strategy was implemented on the basis of Hg^{2+} specific recognition thymine-Hg^{2+}-thymine (T-Hg^{2+}-T)-induced DNA strand displacement. The polystyrene magnetic microspheres coated by AuNPs (Au@PSC) as magnetic separator was labeled with ssDNA D1 (thymine-rich) and S1/D2 DNA duplex (guanine-rich S1) firstly. In the presence of Hg^{2+} and a long ssDNA D3 (thymine-rich at 5' end), the formation of stable T-Hg^{2+}-T structure between D2 and D3 could push S1 out from the S1/D2 DNA duplex, realizing the conversion of input target Hg^{2+} into output S1. Thus, the total amount of output S1 was proportional to the amount of input Hg^{2+}. Thereafter, the output S1 was served as the primer to perform the RCA for obtaining a long guanine-rich ssDNA, which could be further hybridized with the capture DNA on the electrode surface. And then, methyleneblue (MB) as electron mediator interacts with the ssDNA polymers *via* electrostatic binding to produce a detection signal. The electrochemical biosensor exhibited a wide linear range of 1 pM to 1 μM with low detection limit of 0.684 pM. Importantly, this sensor could be successfully applied in water samples with good accuracy and excellent recovery, which provided the potential for Hg^{2+} detection in environment.

Introduction

Mercury, a widespread global pollutant, is one of the most hazardous elements.[1] Typically, the bioaccumulation, bioavailability and toxicity are dependent on its chemical form in living organisms. And Hg^{2+}, is one of the most stable and common forms due to its good water solubility. Hence, Hg^{2+} will be absorbed and then accumulated in living organisms through food chain. Terribly, long-term absorption of Hg^{2+} will result in memory deficit, kidney damage and other health problems.[2-4] Thus, developing reliable, facile, and sensitive methods for efficient routine detection of Hg^{2+} is very necessary. Up to now, many methods have been widely used for Hg^{2+} detection in water samples, including atomic absorption/emission spectroscopy,[5, 6] inductively coupled plasma mass spectrometry,[7, 8] ion chromatography,[9] high-performance liquid chromatography,[10, 11] fluorescence spectrometry,[12, 13] and electrochemical sensing strategy.[14-19] Among them, the Hg^{2+} sensors based on electrochemical method has caused wide concern and be widely applied, because it eliminates the trouble of sophisticated instrumentation, skilled personnel and t*ime consuming sam*ple preparation process.

Protein proximity assay is a DNA-assisted assembly strategy. The key concept in proximity assay is the "proximity effect": a pair of DNA-conjugated affinity probes (antibody) can simultaneously recognize the target protein, subsequently induce the approach and hybridization of DNA labels.[20-22] Thus, the affinity recognition event can be encoded into a convenient DNA "signal" for readout. A few electrochemical proximity immunoassays have been developed for the detection of protein, enzyme, DNA/RNA by combining the proximity hybridization with DNA sensor.[23-31] To the best of our knowledge, however, there is no report focus on proximity hybridization for electrochemical detection of Hg^{2+}. Mercury-sensing strategies based on T-Hg^{2+}-T coordination chemistry have been widely established.[14, 32-39] Inspiringly, it will be significative if the T-Hg^{2+}-T coordination can be taken as antigen/antibody specific recognition to carry out electrochemical proximity hybridization. We can build a high-efficiency converting system to realize the conversion of target Hg^{2+} to ssDNA by proximity hybridization, which can induce further DNA assembly more simply and specifically in view of the steric effect. To improve the sensitivity, a biochemical technique, RCA, has been employed for signal amplification. RCA, a newly developed thermostatic nucleic acid amplification method, is actuated by DNA polymerase and circularized oligonucleotide template with either linear or geometric kinetics through a short DNA primer.[40-44] The products of RCA (ssDNA) can be hundreds or thousands of fold

[a] *Chongqing Key Laboratory of Environmental Materials and Remediation Technologies (Chongqing University of Arts and Sciences), Chongqing University of Arts and Sciences, Chongqing 402160, PR China. E-mail: tangying2282@163.com (Y. Tang); xieshunbi@163.com (S. B Xie); Tel: +86-23-49891739.*
[b] *College of Chemistry and Chemical Engineering, Southwest University, Chongqing 400715, PR China*
Electronic Supplementary Information (ESI) available: The characterization of AuNPs and Au@PSC, The optimization of D3, Polyacrylamide gel electrophoresis

View Article Online
DOI: 10.1039/C7AN01306J

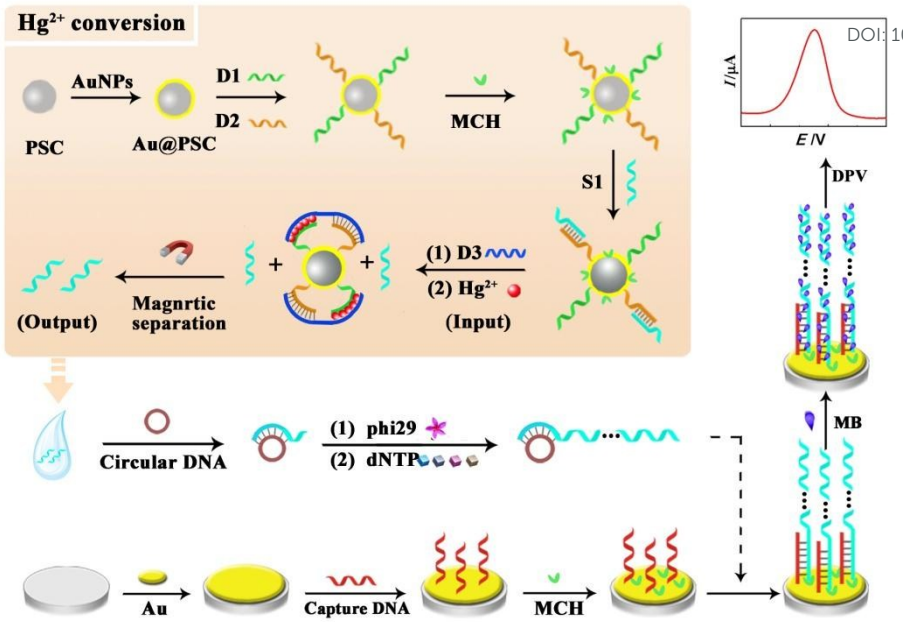

Scheme 1. Schematic illustration of the electrochemical biosensor based on Hg^{2+} converting strategy and rolling circle amplification for Hg^{2+} detection.

longer than the primer，which powerfully increased the detection signals of nucleic acid target sequence.[39, 45, 46]

In this work, we presented a high-efficiency Hg^{2+} converting strategy for ultrasensitive detection of Hg^{2+} based on specific recognition driven DNA strand displacement and the improved rolling circle amplification. The construction and detection principle of the biosensor is illustrated in Scheme 1. First, two single-stranded oligonucleotides D1 and D3 were designed to be thymine-rich for preparation of two affinity probes. In order to realize Hg^{2+} conversion, S1/D2 DNA duplex and D1 were initially immobilized on the surface of Au@PSC via the Au-S bond.[47] In the presence of Hg^{2+} and D3, T-Hg^{2+}-T specific recognition would bring D3 close to the S1/D2 duplex. And then, D3 served as competing DNA to displace S1 from S1/D2 duplex by formation of D2/D3 duplex. As a result, with more Hg^{2+} added, more S1 products would be released. The output S1 was obtained through a magnetic separation process and then used as a primer in the following RCA amplification. At the acceleration of DNA polymerase and circularized template, enormous ssDNA (RCA products) has been generated. The obtained RCA products has been further immobilized on the electrode surface by hybridizing with the capture DNA which assembled on electrode surface. Afterward, a large amount of MB as electron mediator could be interacted with the ssDNA *via* electrostatic binding for achieving a remarkable detection signal. Therefore, the sensitivity of the proposed method could be significantly enhanced by using T-Hg^{2+}-T induced DNA strand displacement and RCA for signal amplification.

Experimental

Materials and apparatus

Standard solution of mercury (GSB04-1729-2004, 1000 μg/mL) was provided by National Center of Analysis and Testing for Nonferrous Metals and Electronic Materials (Beijing, China). 6-mercapto-1-hexanol (MCH), hydrochloroauric acid, tris(2-carboxyethyl)phosphine (TCEP), from Sigma (St. Louis, MO, USA). Amine-modified polystyrene magnetic microspheres (PSC-NH_2) were provided by Tianjin BaseLine ChromTech Research Centre (Tianjin, China). The Bovine serum albumin Fraction V (BSA) was purchased from GenView Sci. Inc. (USA). A phosphate buffer saline (PBS, 100 mM, pH 7.0, containing 100 mM Na_2HPO_4, 100 mM NaH_2PO_4, and 2 mM $MgCl_2$) was used as working buffer solution. The T4 DNA ligase and T4 DNA ligase buffer were purchased from Sangon Biotech. Co., Ltd. (Shanghai, China). The phi29 DNA polymerase and 1 mL 10× reaction buffer (330 mM Tris-acetate (pH 7.9 at 37 °C), 100 mM Mg-acetate, 660 mM K-acetate, 1% (*v*/*v*) Tween 20, 10 mM DTT) were prepared by thermo fisher scientific Inc. (USA). All synthesized oligonucleotides were ordered from Sangon Biotech. Co., Ltd. (Shanghai, China). They were kept at -20 °C for further use. And oligonucleotides sequences were listed in Table 1. Other chemicals were of analytical grade and were used without further purification.

Table 1 *Synthetic oligonucleotide sequences*

Name	Sequences*(5′→3′)
D1	T TTT TTT TTT TTT TTC GAG TC-$(CH_2)_6$-SH
D2	SH-$(CH_2)_6$-TAG TCA GTT AAC CCT CCA CCC CCT CCC ATC
D3	T TTT TTT TTT TTT TTA ATG ACC TAT GAA GGA GGG GGT GGA GG
S1	AGT ACT TCG ATG GGA GGG GGT GGA GG
circular DNA	phosphate-CCACCTCCTAGATGCAACCCTCCC
capture DNA	TCG AAG TAC T-$(CH_2)_6$-SH

View Article Online
DOI: 10.1039/C7AN01306J

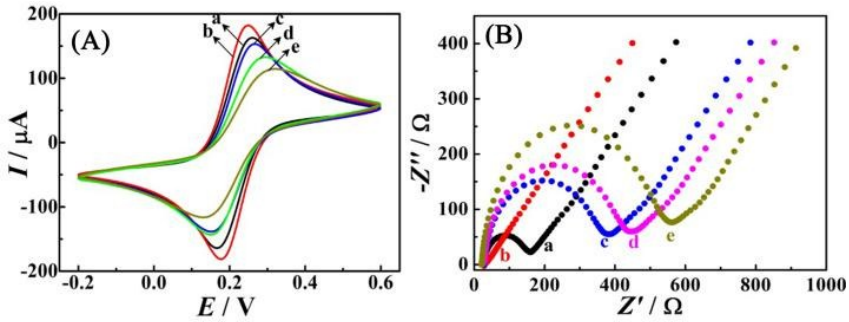

Figure 1. The CV (A) and EIS (B): (a) bare GCE, (b) Au/GCE, (c) capture DNA-Au/GCE, (d)MCH-capture DNA-Au/GCE, and (e) RCA products/MCH-capture DNA-Au/GCE.

Electrochemical measurements were carried out on a CHI660E electrochemistry system (Chenhua Instrument, Shanghai, China). The morphology of Au@Fe3O4 was characterized by scanning electron microscope (SEM, S-4800, Hitachi, Japan). The transmission electron micrograph (TEM) was performed on a Tecnai G2 F20 microscope (FEI Co, U.S.A). The image of the electrophoresis was recorded by Tanon 5200 Multi Chemiluminescent/Fluorescence Image System. The conventional three-electrode system consisted of a glassy carbon electrode (GCE, 4 mm in diameter) as working electrode, an saturated calomel electrode as reference electrode, and a Pt wire as auxiliary electrode. A TGL-185M medical centrifuge (Pingfan Instrument, Changsha, China) was used in the assay. All experiments were performed at room temperature unless otherwise mentioned.

The Synthesis of the S1/D2-Au@PSC-D1 biocomplex

All glassware used in the following procedures was cleaned in a bath of freshly prepared nitrohydrochloric acid (3:1 HCl-HNO_3). Firstly, gold nanoparticles (AuNPs) were prepared by adding 120 μL of 1% (*w*/*w*) sodium citrate solution into 10 mL of 0.01% (*w*/*w*) $HAuCl_4$ boiling solution according to the literature.[48] And the prepared AuNPs suspension was stored in a refrigerator in a dark-colored glass bottle for further use. Thereafter, 1 mL (5 mg/mL) of PSC (surface groups: -NH_2) solution was isolated by magnet and washed with ultrapure water three times. And then, 2 mL synthesized AuNPs were transferred into 1 mL PSC solution, and the mixture was continuously stirred at room temperature for 30 min, the PSC would be coated with a AuNPs layer owing to stable Au-N bond. Subsequently, the magnetic Au@PSC were collected from the solution with a magnet and dispersed again in 1 mL PBS (pH 7.4) to obtain a homogeneous solution. The characterization of AuNPs and Au@PSC were displayed in Electronic Supplementary Information.

After that, 80 μL of PBS containing 40 μL Au@PSC, 20 μL 4 μM thiol-modified single-stranded D1, and 20 μL 4 μM thiolated single-stranded D2 was reacted at room temperature for 12 h. The supernatant was removed by magnetic force, followed by adding 2 mM MCH to block nonspecific binding sites. After a magnetic separation and washing with PBS (pH 7.4), the D1-Au@PSC-D2 could be formed. Then the complementary single-stranded S1 (80 μL, 2 μM) was added into the D1-Au@PSC-D2 solution and incubated for 120 min at 37 °C. the nonhybridized S1 was removed by a magnetic separation. And thus, the S1/D2-Au@PSC-D1 biocomplex has been synthesized

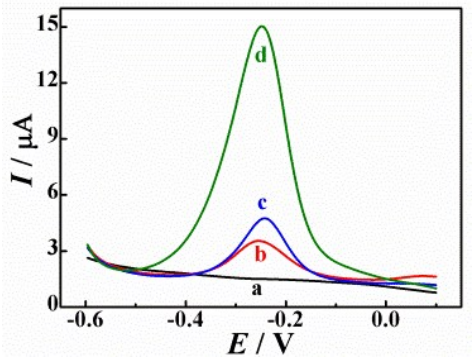

Figure 2. DPV of the different modified electrodes in 10 mL of PBS (pH 7.0) after incubated with 5 μL 1.0 mM MB solution: (a) bare Au/GCE, (b) MCH/capture DNA-Au/GCE, (c) The S1 products/MCH/capture DNA-Au/GCE, (d) The RCA products/MCH/capture DNA-Au/GCE by using 1 μM Hg^{2+} as an example.

The Hg^{2+} conversion and RCA process

First, the S1/D2-Au@PSC-D1 biocomplex was incubated with 10 μL of 8 μM D3 and 10 μL of Hg^{2+} solution with various concentrations at 37 °C for 150 min. Then, 20 μL solutions containing various concentrations of S1 products has been collected with a magnetic field and further used for the RCA.

The typical RCA process was as follows: first, the padlock RCA template were prepared by ligation reaction in 20 μL of buffer containing 1× T4 ligase buffer (6.6 mM $MgCl_2$, 10 mM DTT, 0.1 mM ATP, 66 mM Tris-HCl (pH 7.6)), 1 μM primer (above output S1), 1 μM linear circular DNA, and 50 U T4 ligase at 16 °C overnight after initial denaturation at 95 °C for 5 min. After heating at 60 °C for 20 min to inactivate T4 DNA ligase, the above padlock RCA template were added to 4 μL dNTPs (2.5 mM, dTTP, dATP, dGTP, dCTP), 4 μL phi29 DNA polymerase (10 U/μL in 1× phi29 DNA polymerase buffer, 1 μL bovine serum albumin (BSA, 1×) and 1 μL phi29 DNA polymerase buffer (10×). The mixture was then incubated at 37 °C for 80 min to initiate a RCA process. Finally, the resulting mixture was incubated at 65 °C for 5 min to inactivate the polymerase.

Sensor fabrication and electrochemical measurements

Prior to use, the GCE was polished to obtain a mirror surface on a polishing cloth with 0.3, 0.05 μm alumina slurry respectively, followed by successive sonication in ultrapure water, ethanol for 5 min and dried in air. Subsequently, AuNPs was electrodeposited on the clean GCE in 1% (w/w) $HAuCl_4$ solution containing 0.5 M perchloric acid at a potential of -0.20 V for 30 s. To reduce the formation of the disulfides, the capture DNA was immersed into 10 mM TCEP for 1 h before use. Thereafter, 1 μM of capture DNA was assembled on the Au/GCE for 12 h, then the electrode was treated with 2 mM of MCH for 40 min. The 10 μL guanine-rich RCA products was dropped on the above modified GCE and incubate at 37 °C for 2 h and rinsed with ultrapure water. Finally, MB solution (5 μL, 1.0 mM) was dropped on the RCA products modified GCE and incubate for 1 h at room temperature. Through this process, the MB moleculars could embed into the RCA products via electrostatic adsorption.

Ultimately, differential pulse voltammetry (DPV) was conducted in 10 mL of PBS (pH 7.0). The DPV was carried out between -0.6 V and 0.1 V under pulse amplitude of 25 mV, with a step potential of 4 mV. Optimization of detection conditions, reproducibility, stability and selectivity experiments were performed next. In addition, 1 μM Hg^{2+} was used in all optimization experiments and selectivity measurements.

Results and discussion

Characterization of the biosensor

To further provide information about the preparation of the biosensor, the CV and EIS were used to investigate the stepwise of the electrode modification process. Figure 1A showed the CV of the stepwise modification processes in 5.0 mM $[Fe(CN)_6]^{3-/4-}$. In curve a, the bare GCE exhibited a couple of reversible redox peaks. Then, the peak current increased after AuNPs has been deposited on the bare electrode (curve b). Because the conductivity of AuNPs promoted the electron transfer. Next, the capture DNA has been immobilized on the Au/GCE, the peak current decreased (curve c). Subsequently, MCH was immobilized to block the remaining active sites, and a further decreased peak current was obtained (curve d). Finally, when RCA products were dropped on the modified electrode, the complementary sequence of RCA products hybridized with the capture DNA, the formation of dsDNA polymers could hindered the transmission of electrons towards the electrode surface, therefore, a decrease peak current could be observed (curve e). In order to further prove the sensor assembly process, EIS was used to investigate the interfacial properties of the modified electrode in 5.0 mM $[Fe(CN)_6]^{3-/4-}$. The EIS results （Figure 1B）were consistent with CV results, which testified the successful construction of the sensor.

The Signal Amplification Strategy

To investigate the effects of signal amplification strategy, different signal probes and detection protocols were used to test the same samples and the results were shown in Figure 2. As could be seen from curve a, no redox peak could be observed at the ungroomed Au/GCE. When the Au/GCE was just modified with capture DNA and MCH, the weak signal peaks (curve b) were observed due to the limited guanine in capture DNA; When the MCH/capture DNA-Au/GCE incubated with the outputted S1 products, the current response increased slightly(curve c), because the S1/capture DNA heteroduplex can immobilize more MB; More significantly, the largest current response was obtained from curve d when the MCH/capture DNA-Au/GCE incubated with the RCA products, and the peak value of curve d had remarkable enhance compared to curve c. These results demonstrate the formation of RCA products/capture DNA on the Au/GCE and the successful implementation of RCA signal amplification function.

Optimization of experimental conditions

Before testifying the utility of the sensor for Hg^{2+} detection, relevant experimental parameters were optimized to maximize the performance of the sensor. The output of S1 products refers to the coinstantaneous development about specific binding of D1/D3 and the hybridization of D2/D3. Thus, the incubation time for target Hg^{2+} converting system was optimized in this study. It could be obviously observed that the current intensity enhanced over time and then tended to level off after 150 min, demonstrating that 150 min was enough for the incubation for target Hg^{2+} converting system (Figure 3A). Because RCA process is required to ensure the signal amplification, the effect of the RCA reaction time was also investigated in this experiment. As shown in Figure 3B, the detection signal increased from 20 to 80 min and then reached a plateau, suggesting the reaction was completely finished at 80 min. Thus, the optimal RCA reaction time was 80 min, which has been adopted in the following experiment.

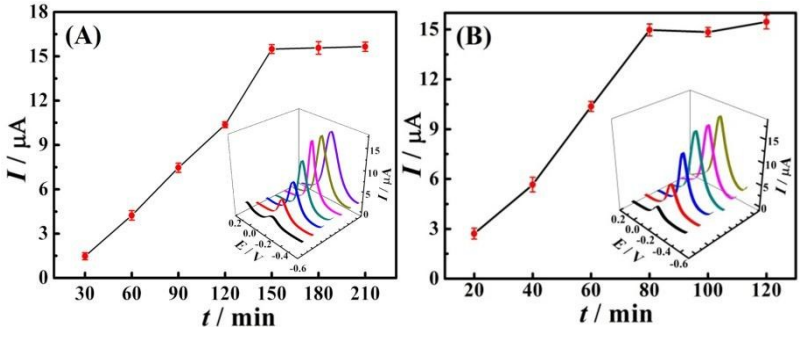

View Article Online
DOI: 10.1039/C7AN01306J

Figure 3. The effects of (A) the incubation time for target Hg^{2+} converting system, and (B) RCA reaction time on peak current of as-prepared sensor by using 1 μM Hg^{2+} as an example.

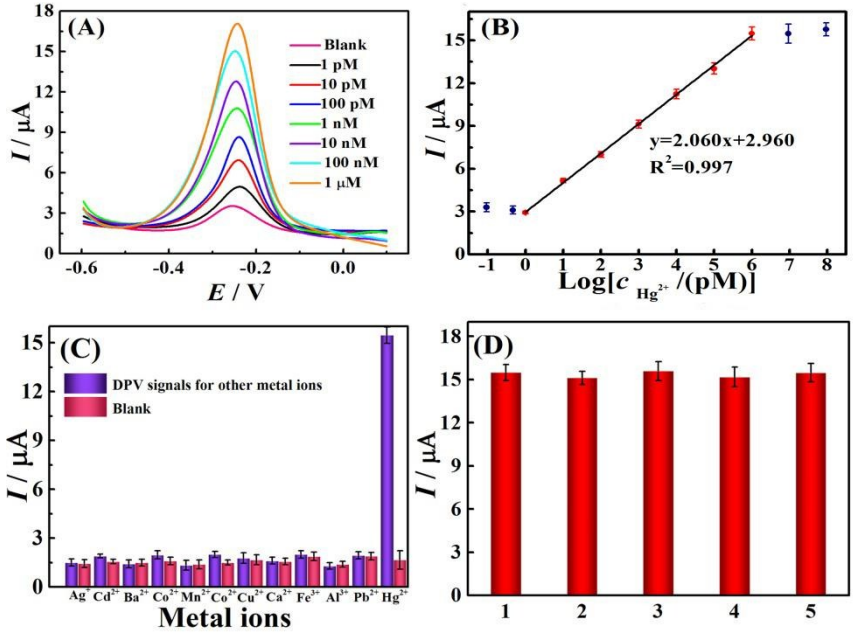

Figure 4. (A) DPV responses of the electrochemical sensing platform toward different-concentration Hg^{2+} standards in pH 7.0 PBS; (B) The linear relationship between the current (I) and the logarithm of Hg^{2+} concentration. (C) Selectivity of the biosensor towards different metal ions; (D) Reproducibility of the proposed biosensor by using 1 μM Hg^{2+} as an example in the same batch.

Table 2. The comparative features of different detection schemes about monitoring Hg^{2+}

Detection method	Linear range	Detection limit	Reference
self-powered triboelectric nanosensor	100 nM - 5μM	30 nM	[49]
mercury-specific oligonucleotide-based electrochemiluminescence biosensor	50 pM - 10 nM	5.1 pM	[50]
gold nanoparticles-based hybrid microgel fluorescent sensor	160 nM - 1.60 μM	31 nM	[51]
N-doped carbon nanodot-based photoluminescent sensor	0.25 μM - 6 μM	80 nM	[52]
phenylamine oligothiophene derivative-based fluorescent sensor	0 μM - 10 μM	439 nM	[53]
hybridization chain reaction-based fluorescent sensor	1.0 nM - 6.0 nM	0.36 nM	[54]
Hg^{2+} converting strategy-based electrochemical biosensor	1.0 pM - 1 μM	0.684 pM	Our work

Detecability of electrochemical sensor

The current response of the sensing method to different concentrations of Hg^{2+} was examined under optimized experimental conditions, and the results were displayed in Figure 4A. The DPV peak current gradually increased with the increasing Hg^{2+} concentration from 1 pM to 1 μM. A good linear relationship (Figure 4B) between the response signal and Hg^{2+} level was obtained, the linear regression equation was I (μA) = 2.060 log ($c_{Hg}{}^{2+}$/pM) + 2.960, (R^2 = 0.997). And the detection limit was evaluated to be 0.684 pM at a signal-to-noise ratio of 3σ (where σ is the standard deviation of a blank sample, n = 11). To further evaluate the advantages of the developed assay, the analytical properties were compared with other reported models (Table 2). Apparently, the limit of detection (LOD) of the proposed biosensor was comparable with those of other Hg^{2+} detection schemes. The proposed biosensor exhibited excellent analytical performance, which should be attributed to the highly effective target converting strategy and RCA signal amplification.

Selectivity and reproducibility of electrochemical sensor

The selectivity of the sensing system was determined by challenging it with other metal ions at 50 μM. As shown in Figure 4C, the DPV signals for other metal ions were as small as the background (in the absence of mercury ions), whereas a significantly higher electrochemical signal was obtained when the biosensor was incubated with 1 μM Hg^{2+}. This excellent selectivity arises from the high specificity of the special Hg^{2+} conversion. In order to estimate the reproducibility (Figure 4D), five independently prepared electrodes were used with the relative standard deviation (RSD) of 1.4%, illustrating the acceptable reproducibility of the electrochemical biosensor.

View Article Online
DOI: 10.1039/C7AN01306J

When stored at 4 °C for a week, the biosensor maintained 91.4% of the initial value. The experimental results indicated that the biosensor has admirable stability for Hg^{2+} detection.

Table 3. Determination of Hg^{2+} in environmental tap water samples using the proposed method

Sample	Added (nM)	Found (mean[a] ± SD[b]) (nM)	Recovery (%)
tap water 1	0.05	0.048 ± 0.003	99.3%
tap water 2	0.1	0.097 ± 0.002	99.0%
tap water 3	5.0	5.02 ± 0.18	100.4%

[a] **Mean of three determinations;** [b] **SD, standard deviation;** [c] **No Hg^{2+} could be detected.**

Environmental samples analysis

To evaluate the possible application of our strategy for real samples, the tap water samples spiked with different concentrations of Hg^{2+} were detected according to the foregoing procedure with three replicates. The results were summarized in Table 3. Satisfactory values between 99% and 100.4% were obtained for the recovery experiments, which are in the acceptable ranges for real sample assay. The above results demonstrated that the developed biosensor has great application potential for Hg^{2+} detection in real water samples.

Conclusions

In summary, we successfully developed a electrochemical sensor for detection of Hg^{2+}: (1) the sensor contains a target Hg^{2+} converting system based on T-Hg^{2+}-T specific binding-driven DNA strand displacement. Therefore, Hg^{2+} detection could be converted to the DNA assay which extends the method for metal ions detection from the traditional immunoassay; (2) the sensor also contains a rolling circle amplification process to amplify the signal response. This RCA-based sensing system does not require complicated thermal cycling steps or ligation steps, and shows a promising potential for on-site testing with ultra-low detection limit (0.684 pM) and wide linear range (1 pM-1 μM). Our strategy could meet the needs of EPA (United States Environment Protection Agency) guideline for Hg^{2+} detection in tap drinking water (≤10 nM).[55-57] Also, our system exhibited good selectivity against other metal ions. Importantly, this approach could be successfully applied in real samples, which provided the potential for Hg^{2+} detection in in real water samples.

Acknowledgements

This work was financially supported by the NNSF of China (21705013), the Chongqing Science and Technology Commission of China (cstc2017jcyjAX0282, cstc2015jcyjBX0126, cstc2016shmsZX20001), the Science and Technology Research Program of Chongqing Municipal Education Commission China (KJ1711265), The Foundation for High-level Talents of Chongqing University of Arts and Sciences, China (R2016CH08).

References

1. C.-T. Driscoll, R.-P. Mason, H.-M. Chan, D.-J. Jacob and N. Pirrone, *Environ. Sci. Technol.*, 2013, **47**, 4967-4983.
2. Y. Wang, F. Yang and X. Yang, *Biosens. Bioelectron.*, 2010, **25**, 1994-1998.
3. E.-M. Nolan and S.-J. Lippard, *Cheminform.*, 2008, **108**, 3443-3480.
4. F. Zahir, S.-J. Rizwi, S.-K. Haq and R.-H. Khan, *Environ. Toxicol. Phar.*, 2005, **20**, 351-360.
5. M.-M.-L. Guerrero, M.-T.-S. Cordero, E.-V. Alonso, A.-G.-D. Torres and J.-M.-C. Pavón, *Microchem. J.*, 2017, **132**, 274-279.
6. M.-A. Kamyabi and A.-Aghaei, *Spectrochim. Acta, Part B,* 2017, **128**, 17-21.
7. S. Ma, M. He, B. Chen, W. Deng, Q. Zheng and B. Hu, *Talanta*, 2016, **146**, 93-99.
8. Y. Chen, X. Cheng, F. Mo, L. Huang, Z. Wu, Y. Wu, L. Xu and F. Fu, *Electrophoresis*, 2016, **37**, 1055-1062.
9. Q. Liu, *Microchem. J.*, 2010, **95**, 255-258.
10. S. Zhang, H. Luo, Y. Zhang, X. Li, J. Liu, Q. Xu and Z. Wang, *Microchem. J,*, 2016, **126**, 25-31.
11. T. Wei, T. Dong, Z. Wang, J. Bao, W. Tu and Z. Dai, *J. Am. Chem. Soc.*, 2015, **137**, 8880-8883.
12. L. Lan, Q. Niu, Z. Guo, H. Liu and T. Li, *Sens. Actuators, B*, 2017, **244**, 500-508.
13. X. Wu, J. Chen and J.-X. Zhao, *Analyst*, 2013, **138**, 5281-5287.
14. Y. Zhang, G.-M. Zeng, L. Tang, J. Chen, Y. Zhu, X.-X. He, Y. He and A. Chem, *Anal. Chem.*, 2015, **87**, 989-996.
15. L. Z, *Biosens. Bioelectron.*, 2016, **80**, 339-343.
16. J. Chen, S. Zhou and J. Wen, *Anal. Chem.*, 2014, **86**, 3108-3114.
17. Y. Zhao, L. Xu, S. Li, Q. Chen, D. Yang, L. Chen and H. Wang, *Analyst*, 2015, **140**, 1832.
18. N. Zhou, J. Li, H. Chen, C. Liao and L. Chen, *Analyst*, 2013, **138**, 1091-1097.
19. N. Zhou, H. Chen, J. Li and L. Chen, *Microchim. Acta.*, 2013, **180**, 493-499.
20. T.-Z. Gómez, R. Ke, A. Mezger, P. Svedlindh, M. Strømme and M. Nilsson, *Small*, 2012, **8**, 2174-2177.
21. R.-Y. Nong, D. Wu, J. Yan, M. Hammond, G.-J. Gu, M. Kamali-Moghaddam, U. Landegren and S. Darmanis, *Nat.*

Protoc., 2015, **10**, 1234-1248.
22. M. Zou, D. Li, R. Yuan and X. Yun, *Biosens. Bioelectron*., 2017, **92**, 624-629.
23. Y. Yuan, G. Liu, Y. Chai and R. Yuan, *Sens. Actuators, B*, 2017, **246**, 402–407.
24. F. Zhou, Y. Yao, J. Luo, X. Zhang, Y. Zhang, D. Yin, F. Gao and P. Wang, *Anal. Chim. Acta.*, 2017, **969**, 8-17.
25. Y. Qian, T. Fan, P. Wang, X. Zhang, J. Luo, F. Zhou, Y. Yao, X. Liao, Y. Li and F. Gao, *Sens. Actuators, B*, 2017, **248**, 187-194.
26. F. Gao, T. Fan, W. Jing, L. Sha, D. Yan, Y. Yao, F. Zhou, Z. Yu, X. Liao and D. Geng, *Biosens. Bioelectron*., 2017, **96**, 62-67.
27. J. Hu, T. Wang, J. Kim, C. Shannon and C. J. Easley, *J. Am. Chem. Soc.*, 2012, **134**, 7066-7072.
28. J. Hu, Y. Yu, J.-C. Brooks, L.-A. Godwin, S. Somasundaram, F. Torabinejad, J. Kim, C. Shannon and C.-J. Easley, *J. Am. Chem. So.*, 2014, **136**, 8467-8474.
29. Z.-H. Yang, Y. Zhuo, R. Yuan and Y.-Q. Chai, *Anal. Chem.*, 2016, **88**, 5189-5196.
30. Y. Zhang, Y. Wang, H. Wang, J.-H. Jiang, G.-L. Shen, R.-Q. Yu and J. Li, *Anal. Chem.*, 2009, **81**, 1982-1987.
31. Y.-L. Zhang, Y. Huang, J.-H. Jiang, G.-L. Shen and R.-Q. Yu, *J. Am. Chem. Soc.*, 2007, **129**, 15448-15449.
32. J. Zhuang, L. Fu, D. Tang, M. Xu, G. Chen and H. Yang, *Biosens. Bioelectron*., 2013, **39**, 315-319.
33. H.-C. Chan, J.-H. Kim, J. Jung and B.-H. Chung, *Biosens. Bioelectron*., 2013, **41**, 827–832.
34. Y. Zhu, P. Liu, X.-H. Yang, L.-L.He, Q.-Z. Li, Q. Wang, K. M. Wang, J. Huang and J. B. Liu, *Chemical Journal of Chinese Universities*, 2012, **33**, 2651-2656.
35. G. Morpiperberg, T.-V. Ran, J. Elbaz and I. Willner, *J. Am. Chem. Soc.*, 2010, **132**, 6878-6879.
36. B. Zhang and L.-H. Guo, *Biosens. Bioelectron*., 2012, **37**, 112-115
37. J. Tang, Y. Yu, H. Shi, X. He, Y. Lei, J. Shangguan, X. Yang, Z. Qiao and K. Wang, *Anal. Chem.*, 2017, **89**, 6637-6644.
38. F. Wang, L. Freage, R. Orbach and I. Willner, *Anal. Chem.*, 2013, **85**, 8196-8203.
39. Z. Qiu, J. Shu, G. Jin, M. Xu, Q. Wei, G. Chen and D. Tang, *Biosens. Bioelectron.*, 2016, **77**, 681-686.
40. P.-M. Lizardi, X. Huang, Z. Zhu, P. Brayward, D.-C. Thomas and D.-C. Ward, *Nat. Genet.*, 1998, **19**, 225-232.
41. B. Schweitzer, S. Roberts, B. Grimwade, W. Shao, M. Wang, Q. Fu, Q. Shu, I. Laroche, Z. Zhou and V.-T. Tchernev, *Nat. Biotechnol.*, 2002, **20**, 359-365.
42. F.-B. Dean, J. R. Nelson, T.-L. Giesler and R.-S. Lasken, *Genome. Res.*, 2001, **11**, 1095-1099.
43. B. Schweitzer, S. Wiltshire, J. Lambert, S. O'Malley, K. Kukanskis, Z. Zhu, S. F. Kingsmore, P. M. Lizardi and D.-C. Ward, *Proc. Natl. Acad. Sci. U. S. A.*, 2000, **97**, 10113-10119.
44. Q. Xue, Y. Lv, Y. Zhang, S. Xu, Q. Yue, R. Li, L. Wang, H. Li, X. Gu and S. Zhang, *RSC Adv.*, 2014, **4**, 27091-27097.
45. U-B. Gyllensten and H.-A. Erlich, *Proc. Natl. Acad. Sci. U. S. A.*, 1988, **85**, 7652-7656.
46. E.-Y. Loh, J.-F. Elliott, S.-Cwirla, L.-L. Lanier and M.-M. Davis, *Science*, 1989, **243**, 217-220.
47. K. Zhang, S. Lv, Z. Lin and D. Tang, *Biosensors & Bioelectronics*, 2017, **95**, 34.
48. G. Frens, *Nature*, 1973, **241**, 20-22.
49. Z.-H. Lin, G. Zhu, Z.-Y. Sheng, Y. Yang, B. Peng, J. Chen and W.-Z. Lin, *Angew. Chem. Int. Ed*, 2013, **52**, 5065-5069.
50. R.-F. Huang, H.-X. Liu, Q.-Q. Gai, G.-J. Liu and Z. Wei, *Biosens. Bioelectron.*, 2015, **71**, 194-199.
51. Y. Tang, Y. Ding, T. Wu, L. Lv and Z. Yan, *Sens. Actuators, B*, 2016,**228**, 767-773..
52. L. Wang, B. Li, F. Xu, X. Shi, D. Feng, D. Wei, Y. Li, Y. Feng, Y. Wang and D. Jia, *Biosens. Bioelectron*., 2016, **79**, 1-8.
53. Q. Niu, X. Wu, S. Zhang, T. Li, Y. Cui and X. Li, Spectrochim. Acta, Part A, 2016, **153**, 143-146.
54. X. Lv, W. Wu, C. Niu, D. Huang, X. Wang, and X. Zhang, *Talanta*, 2016, **151**, 62-67.
55. S. Pramanik and P. -S. Devi, *New. J. Chem.*, 2017, **41**, 10851-10859.
56. J. Chen, J. Pan and S. Chen, *Chem. Commun.*, 2017, **53**, 10224-10227.
57. M. Hong, M. Wang, W. Jing, X. Xu and Z. Lin, *Biosens. Bioelectron.*, 2017, **94**, 19-23.